Anbar Journal of Engineering Science (AJES) **Vol. 12 , No. 2 (2021) , pp. 100 ~112**
P-ISSN: 1997-9428; E-ISSN: 2705-7440 DOI:10.37649/aengs.2021.171162

Anbar Journal Of Engineering Science©

journal homepage: http://www.uoanbar.edu.iq/Evaluate/

Univiersty of Anbar

Performance of a double-pipe heat exchanger with different metal foam arrangements

Thaer H. Farhan[a*], Obaid T. Fadhil [b], Hamdi E. Ahmed [b]

[a] Communication Office, Khalidia, 31001, Iraq
[b] *Department of Mechanical Engineering, University of Anbar, Ramadi, 31001, Iraq*

PAPER INFO

Paper history:
Received 02/06/2021
Revised 09/08/2021
Accepted 16/08/2021

Keywords:
Annulus heat exchanger; Metal foam arrangement; Full-filled; Partially/periodically-filled; Heat transfer enhancement.

ABSTRACT

This paper contributes to the field of improving the performance of heat exchangers using metal foam (MF) full-filled and partially/periodically-filled within the gap between the two pipes. The effect of configuration and arrangement of copper MF (15PPI and porosity of 0.95) installed on the outer surface of the inner pipe of a counter-flow double-pipe heat exchanger on the thermal and hydraulic performance was studied experimentally. The test section consisted of concentric two pipes; the inner pipe which was made of copper while the outer pipe was a Polyvinyl chloride. Air was used as a working fluid in both hot and cold sides. A wide cold air flow rate range was covered from 3 to 36 m^3/h which corresponds to Reynolds number (*Re*) range from 2811 to 31,335. The hot air flow rate was kept constant at $3m^3/h$. The temperature difference (ΔT) between the inlet hot air and inlet cold air was adopted to be (20°C, 30°C, 40°C, and 50°C). The results revealed that the higher Nusselt number (Nu) was at ΔT= 50°C and the thermal performance of the heat exchanger with the MF for all the arrangements was greater than the smooth heat exchanger. The highest and lowest friction factor was 1.033 and 0.0833 for the case 1 and 8, respectively, and the optimal performance evaluation criteria (PEC) was 1.62 for case 7 at Re = 2800. The Nu would be increased with a moderate increase in the friction factor by optimizing the arrangement of the MF. The two essential parameters that played an important role for increasing the PEC were the MF diameter and the MF arrangement along the axial length of the cold air stream.

1. Introduction

There are several types of heat exchangers, and they are widely used in various fields for the purpose of dispersing or transferring heat from a hot fluid or object to another cold. The double-pipe heat exchanger is a common type used in industry as well as in thermal plants [1].

Researchers have worked and are still working on improving the performance of the heat exchangers in general and the double-pipe heat exchangers in particular, using various technologies. Metal foam is one of the modern technologies that attracted the attention of researchers.

The effect of inserting copper metal foam fins with an inclination angle of (30°) with the flow direction on the heat transfer and pressure drop in a double-pipe heat exchanger was investigated experimentally by Hamzah and Nima [1]. They claimed that there was a small increase in the pressure drop when the metal foam used. For the counter-flow mode, a higher convection heat transfer coefficient was observed, and this increment increased with increasing Reynolds number. Targui and Kahalerras [2] studied numerically the heat transfer and flow characteristics in a double-tube heat exchanger by installing porous structures within the gap between the two pipes in two stages, one on the outer surface of the inner pipe and the other stage on the inner surface of the outer pipe and on the outer surface of

* Corresponding author. : Thaer H. Farhan ; : thar.farhan@uoanbar.u.iq ; +9647804948519

the thinner pipe in an overlapping manner. The optimal thermal design obtained was when the porous structures used on the inner surface of the outer pipe and on the outer surface of the inner pipe. Also, the heat transfer rate was increased when the thickness of the porous structure increased and, therefore, the distances were reduced. A numerical study was carried out by Kahalerras and Targui [3] to show the effect of porous fins fixed on the outer surface of the inner pipe in a double-pipe heat exchanger on the heat transfer and fluid flow. The fin height, fins spacing and the ratio of the thermal conductivity were the key parameters. It was shown that the heat transfer of the suggested design could be enhanced compared to the traditional one. In addition, the geometry of the fin and each of the thermodynamic and physical properties played an important role in the heat transfer improvement. A numerical study was conducted by Jamarani et al. [4] on a counter-flow double-pipe heat exchanger under turbulent flow condition. The optimum non-dimensional thickness of the porous material which provided higher thermal performance was 0.7 when the porous media installed at the center of the inner pipe and on the inner surface of the outer pipe. Whereas the optimum thickness was 0.4 for the arrangement in which the porous material was fixed at the inner and outer surfaces of the inner pipe. Abbas et al. [5] conducted an experimental study on a double-pipe heat exchanger having semi-circular, circular, and spiral carousel fins fixed on the outer surface of the inner pipe. The convection heat transfer coefficient was improved up to 260% when the fins used at the inner pipe compared to the smooth case. Maid et al. [6] carried out an experimental investigation on a double-tube heat exchanger by placing a metal pad in the inner tube to find out its effect on heat transfer and pressure drop. The factor of enhancement in the convection heat transfer coefficient was 2.074 and the increase in effectiveness was 26.5% as compared to that without metal pad. To find out the effect of the distance between the baffles as well as the fluid flow rate on the effectiveness of a double-pipe heat exchanger, Mishra and Nayak [7] conducted a practical study in which they placed triangular baffles on the outer surface of the inner pipe. They concluded that the effectiveness of the heat exchanger increased as the distance between the baffles decreased and the cold fluid flowrate increased.

Nawaz et al. [8] investigated experimentally the effect of copper and aluminum metal foams on the heat exchanger performance. They found that there was more than one factor of the geometry of the metal foam that affected the amount of pressure drop and heat transfer. Also, the hydrothermal performance with metal foams was higher than that with louver-fin. Xu et al. [9] studied numerically heat transfer in a double-tube heat exchanger with metal foam filling the inner tube and the annulus. They stated that the porosity and pore density should be less than 0.9 and greater than 10 PPI, respectively, to achieve an effectiveness greater than 0.8.

Sertkaya et al. [10] studied experimentally the thermal performance of two heat exchangers; one had aluminum finned tubes, while the second had tubes covered with aluminum foam under turbulent flow regime. They concluded that the heat transfer rate of the finned tube exchangers was greater than that those tubes covered with aluminum foam. Al husseny and Turan [11] installed a layer of metal foam on the connecting surface between the two pipes in order to enhance the thermal conductivity. The heat exchanger was partly filled with a layer of metal foam with a high porosity and rotating coaxially. They demonstrated that the heat transfer can be further enhanced and save pumping energy compared to fully filled heat exchangers.

From the above open literatures, it can be observed that studying the metal foam in several configurations and arrangements inside the annular spacing of the double-pipe heat exchanger is not explored yet. The main goal of the present work is to enhance the heat transfer of a counter-flow double-pipe heat exchanger by inserting metal foam in different arrangements and configurations in the annular space to reduce the fuel required for heating the cold air entering the combustion chamber of power plants. From the view point of the proposal makers, there is no publication that has studied the effect of the arrangement of full filled and partially/periodically filled in the double-pipe heat exchanger yet.

2. Experimental apparatus

The experimental setup used in the present study consisted of the test section (double pipe heat exchanger), two blowers for forcing the hot and cold air, two flow meters for measuring the air flow rates on the hot and cold sides, inclined manometer to measure the pressure difference across the cold air stream for smooth annulus, U-tube manometer to measure the pressure drop across the cold air stream filled with MF, thermocouples to measure the inlet and outlet air temperature at the hot and cold side and the heated wall temperature of the copper cylinder which were connected to a precise digital thermometer, electrical heating system, and

power supply with controls as shown in the illustrative schematic diagram in Figure. 1(a) and in the photograph Figure. 1(b)

No	details
1	Cold air blower
2	Hot air blower
3	Air heating system
4	Cold Air flow meter
5	Hot Air flow meter
6	Digital display
7	Thermocouples
8	Gate valve
9	Metal foam
10	U-Tube manometer
11	Selector switch
12	Power supply
13	voltmeter and ammeter
14	Bypass
15	Test section
16	Insulator
17	Heater 1000 W
18	Outer pipe (PVC)
19	Inner pipe (copper)

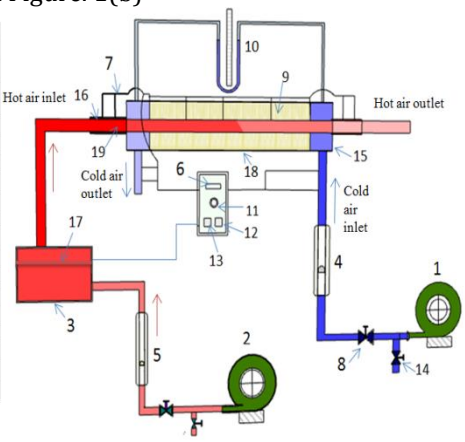

a

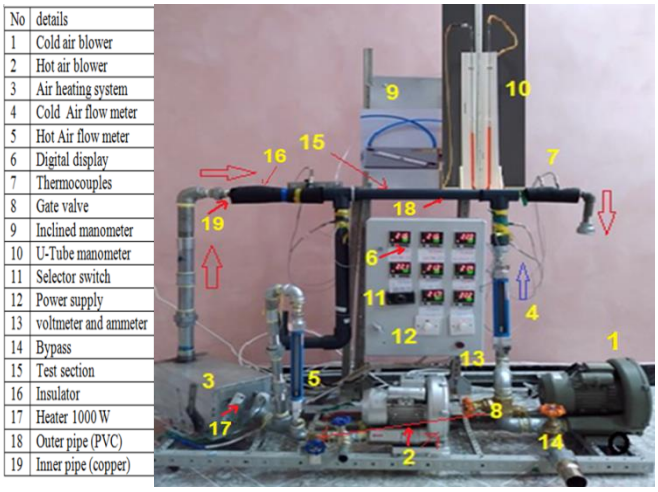

b

Figure 1. The experimental apparatus; (a) schematic diagram, and (b) photog1raph.

2.1. Test rig and instruments

The rig consisted of two concentric pipes where the side view is shown in Figure. 2. The inner pipe of copper and the outer pipe of PVC, which were assembled together by connectors. The inner pipe has an inner diameter of (di¬=17 mm) and an outer diameter (do=19 mm) and the outer pipe has an internal diameter of (Di¬=43 mm), while the hydraulic diameter of the annulus was (Dh=23 mm). The length of the test section was (L=500 mm), whereas the metal foam was installed along the test section. The entry and exit of cold air is through two holes with a diameter of (37.5mm), at the beginning and end of the PVC pipe. Two small holes were drilled at the upstream and downstream end of the annulus with a diameter of (5 mm) in order to connect the manometer flexible tubes.

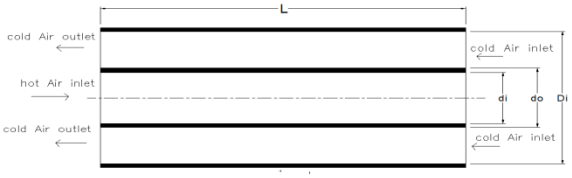

Figure 2. Schematic diagram of the side view of the annular test section.

The cold air blower (OFFICINE AUGUSTO CATTANI, ITALY) with power consumption of (750W) was used to force the cold air within the gap between the two pipes. The hot air blower (OFFICINE AUGUSTO CATTANI, ITALY) with a power consumption of (370W), speed (2800 rpm) was used as well. The amount of cold and hot air was controlled manually by adjusting the valves and the air volumetric flowrate was determined by air flowmeters. The cold air flowrate was measured by a rotary flowmeter, type (VA1OS-25) with a range of 3–50 m^3/h, and accuracy of ±5% which was installed before the test section. The amount of hot air was measured by another rotary flowmeter (VA10S-15) with a range of 1.2–12 m^3/h, and accuracy of ±5%, which was fixed before the heating system. The pressure drop of the smooth annulus was measured by using an inclined manometer due to low pressure drop across the test section. For other cases when the metal foam was installed inside, a U-tube manometer with a range of (0–1200 mm H2O) was used due to high pumping power required. The temperatures were measured by utilizing 13 thermocouples type-K. At each of the entrance and exit of the of the hot air stream, two thermocouples were installed in order to estimate the average temperature of the inlet and outlet hot air, respectively. The probe is inside the hot air duct. By the same way, two thermocouples were installed at the cold air inlet and two thermocouples were installed at the cold air outlet for the same purpose. Also, five thermocouples were fixed on the outer surface of the inner pipe evenly by making a small V-shaped groove in which the probe of the thermocouples was attached inside. The distribution of the thermocouples is shown in Figure. 3. The measurements of temperature were displayed by using digital displays of (Maxwell, MTD-72, accuracy of ±0.3 % FS) and using of selector switch type (TEMPCON).

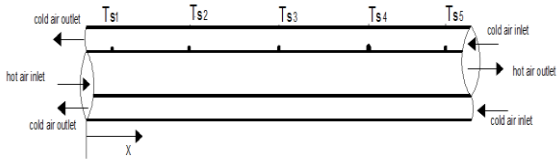

Figure 3 Schematic diagram of thermocouples distribution on the outer surface of the copper pipe.

2.2. Metal foam forming and arrangement

The copper metal foam was cut into concentric washers with a thickness of 10 mm and different diameters according to the arrangements required for doing the tests as shown in Table 1. The arrangements and configurations of the metal foam washers is shown in Figure 4 and photographs shown in Figure 5.

Case NO.	(DMF/D pipe)	Number of MF pieces	Description
1	1	50	The annular space is completely filled with MF, as shown in Figure.(4.a)
2	1	25	The annular space is half fill with MF as shown in Figure.(3.b)
3	0.75	50	The MF covered entire annular space at a height of 75% of the annular space, as shown in Figure.(4.c)
4	1	25	The MF installed periodically in the annular space , as shown in Figure.(4.d)
5	1	13	The MF is gradually placed inside the annular space , as shown in Figure.(4.e)
	0.75	13	
	0.5	12	
	0.25	12	
6	1	12	The MF is installed inside the annular space, as shown in Figure.(4.f)
	0.75	12	
	0.5	12	
	0.25	12	
7	1	7	The MF is installed inside the annular space, as shown in Figure.(4.g)
	0.75	14	
	0.5	14	
	0.25	15	
8	0.0	Without MF	The annular space is empty (smooth), as shown in Figure.(4.h).

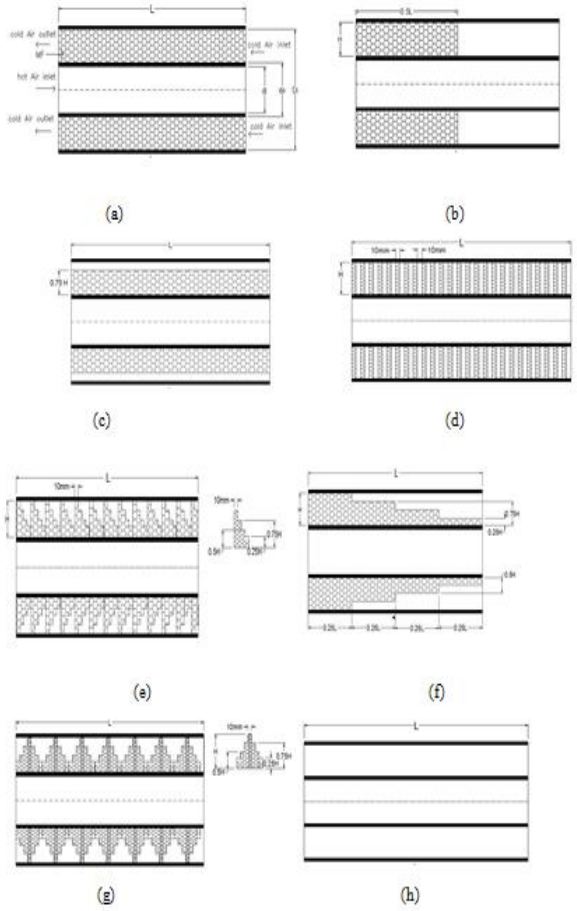

Figure 4. Arrangements and configurations of the metal foam along the annular test section.

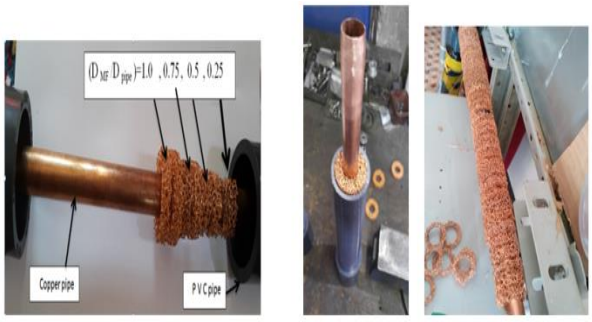

Figure 5. Photographs of the metal foam used in the experiments.

2.3. Test procedure

The following steps represent the procedure of the experiments.

1. The two blowers were turned on first. The power supply of the heaters in the heating system is switch on and the voltage and current are adjusted according to the require air bulk temperature at the inlet of hot side.

2. The air flowrate of the hot and cold side were controlled by adjusting the valves of the blowers. The cold air flowrate was varied according to the requirement of the test, while the hot air flow rate was keep constant.

3. The system was left to work until the cold and hot air temperatures became steady state.

4. The temperature of the hot and cold air at the inlet and outlet, copper surface temperatures, pressure head, and the flow rates of both cold and hot air were measured and recorded.

5. Changing the cold air flowrate (Re) and repeating steps (1– 4).

6. Changing the metal foam arrangement and repeating the steps (1–5).

7. The temperature difference (ΔT) was also changed each time (20, 30, 40, and 50 °C), for three cases only; 1, 2, and 8.

3. Variable parameters calculations

The mass flowrate of air was estimated from the following equation [12]

$$\dot{m}=\dot{V}\times\rho_{air} \quad (1)$$

where $\dot{m}$ is the air mass flowrate (kg/s), $\dot{V}$ is the air volumetric flowrate (m^3/s), and ρ: indicates the density of air (kg/m^3).

The Reynolds number was estimated using the following equation [12]

$$Re = \frac{4\dot{m}}{\pi D_h \mu} \quad (2)$$

The heat transfer from the hot air stream to the cold air stream was calculated according to the following procedure:

- Heat transfer from the hot air is given by [13]

$$Q_h = \left(\dot{m}C_p\right)_h (T_{hi} - T_{ho}) \quad (3)$$

- Heat transfer to cold air is given by [13]

$$Q_c = \left(\dot{m}C_p\right)_c (T_{co} - T_{ci}) \quad (4)$$

The average heat transfer rate (Q_{avg}) between the hot and cold streams is [14]

$$Q_{avg} = \frac{Q_c + Q_h}{2} \quad (5)$$

The heat loss (Q_{loss}) through the test section was calculated as follows [13]:

$$Q_{loss} = Q_h - Q_c \quad (6)$$

The convection heat transfer coefficient of the hot air stream (h_h) was calculated usng the following equation [13]:

$$h_h = \frac{Q_{avg}}{A_i\left(T_{h\ avg} - T_{s_{avg}}\right)} \quad (7)$$

The average temperature of the cold air,

T_(c.avg), and hot air, T_(h.avg) was estimated as follows, respectively [13]

$$T_{h.avg} = \frac{(T_{hi}+T_{ho})}{2} \quad (8)$$

$$T_{c.avg} = \frac{(T_{ci}+T_{co})}{2} \quad (9)$$

The average surface temperature of the copper pipe, $T_{s_{avg}}$ was determined by [12]

$$T_{s_{avg}} = \frac{T_{s_1}+T_{s_2}+T_{s_3}+T_{s_4}+T_{s_5}}{5} \quad (10)$$

The log mean temperature difference, ΔT_LM, can be determined from the following formula [13]

$$\Delta T_{LM} = \frac{(T_{hi}-T_{co})-(T_{ho}-T_{ci})}{\ln[(T_{hi}-T_{co})/(T_{ho}-T_{ci})]} \quad (11)$$

The overall heat transfer coefficient U_i was calculated as follows [12]

$$U_i = \frac{Q_{avg}}{A_i \Delta T_{LM}} \quad (12)$$

where: $A_i = \pi\ L\ d_i$

The hydraulic diameter, D_h, of the annulus was found from

$$D_h = D_i - d_o \quad (13)$$

The convection heat transfer coefficient of cold air, h_c, was calculated from the overall thermal resistance [13]:

$$h_c = \frac{\mathbf{1}}{A_o\left(\frac{\mathbf{1}}{\boldsymbol{UiAi}} - \frac{\mathbf{1}}{h_h \boldsymbol{Ai}} - \frac{\mathbf{ln}\left(\frac{\boldsymbol{do}}{\boldsymbol{di}}\right)}{\mathbf{2\pi KL}}\right)} \quad (14)$$

where $A_o = \pi\ L\ d_o$. The formula of the average Nussle number on the outer surface of the inner cylinder is [15]

$$Nu = \frac{h_c\ D_h}{k} \quad (15)$$

The pressure drop in the annular stream was calculated from [12]

$$\Delta P = \rho_{water} \times g \times \Delta h \quad (16)$$

The friction factor (f) was calculated for the cold air stream from [13]

$$f = \frac{2\ \Delta P\left(\frac{D_h}{L}\right)}{\rho u^2} \quad (17)$$

The effectiveness of the double-pipe heat exchanger (E) was estimated from [1]

$$E = \frac{Q_{ave}}{Q_{max}} \quad (18)$$

The maximum heat transfer can be given as [1]

$$Q_{max} = \left(\dot{m}C_p\right)_h \left(T_{h,i} - T_{c,i}\right) \quad (19)$$

The Performance Evaluated Criteria, PEC, of the double-pipe heat exchanger was found by [13]

$$PEC = \left(\frac{Nu_{MF}}{Nu_s}\right) / \left(\frac{f_s}{f_{MF}}\right)^{1/3} \quad (20)$$

It is worth mentioning that the hot and cold air properties were estimated by using the following correlations which were correlated from the data of air properties published by [16] for a wide range of temperature (0–100) °C. The unit of temperature used in these equations is °C.

$$k = 2.36 \times 10^{-2} + 7.59 \times 10^{-5} \times T_{avg} - 3.39 \times 10^{-8} \times T_{avg}^2 + 1.33 \times 10^{-10} \times T_{avg}^3 - 6.16 \times 10^{-13} \times T_{avg}^4 \quad (21)$$

$$Cp = 1.01 \times 10^3 + 1.49 \times 10^{-1} \times T_{avg} - 4.19 \times 10^{-3} \times T_{avg}^2 + 4.52 \times 10^{-5} \times T_{avg}^3 - 1.44 \times 10^{-7} \times T_{avg}^4 \quad (22)$$

$$\mu = 1.73 \times 10^{-5} + 4.75 \times 10^{-8} \times T_{avg} + 4.58 \times 10^{-11} \times T_{avg}^2 - 2.96 \times 10^{-12} \times T_{avg}^3 + 5.00 \times 10^{-13} \times T_{avg}^4 - 3.84 \times 10^{-16} \times T_{avg}^5 + 1.09 \times 10^{-18} \times T_{avg}^6 \quad (23)$$

$$\rho = 1.2918369 - 4.69 \times 10^{-3} \times T_{avg} + 1.53 \times 10^{-5} \times T_{avg}^2 - 3.03 \times 10^{-8} \times T_{avg}^3 + 4.99 \times 10^{-12} \times T_{avg}^4 \quad (24)$$

4. Uncertainty Analysis

Uncertainties of the experiments have been calculated for parameters such as the Nusselt number, Reynolds number, and friction factors using the Kline and McClintock method [17]. Given a dependent parameter;

$$R = R(X_1 + X_2 + X_3 + \cdots \ldots + X_n) \quad (25)$$

where X_1, X_2, X_3,〖 and X_n are independent measured parameters. Therefore, the uncertainty of R can be calculated as follows

$$U_R = \sqrt{\left(\frac{\partial R}{\partial X_1} U_{X_1}\right)^2 + \left(\frac{\partial R}{\partial X_2} U_{X_2}\right)^2 + \left(\frac{\partial R}{\partial X_3} U_{X_3}\right)^2 + \cdots + \left(\frac{\partial R}{\partial X_n} U_{X_{n1}}\right)^2} \quad (26)$$

where U_{x1}, U_{x2}, U_{x3} and U_{xn} are the uncertainties of independent parameters.

The partial $\frac{\partial R}{\partial X_1}, \frac{\partial R}{\partial X_1}, \frac{\partial R}{\partial X_1}$, and $\frac{\partial R}{\partial X_1}$ are estimated from eq. (25)

Table 2. Uncertainty results

Independent parameter	Accuracy
Volumetric flow rate of air	±5.0%FS , 1.8 m3/h
Air temperature	±0.93%
Pressure head, Δh	±1mm

5. Verification

The current study is first verified before doing the tests for the Nu number, Figure 6 (a), and friction factor, Figure 6 (b), by making a comparison with the data published by Thejaraju et al. [13] and Blasius's correlation for friction factor of smooth pipe over a wide range of Reynolds number. The deviation of the Nusselt number between the current study and [13] is ±7.4%, while the deviations of the friction factor with the Blasius's correlation and [13] are ±7.6%, ±9.2%, respectively.

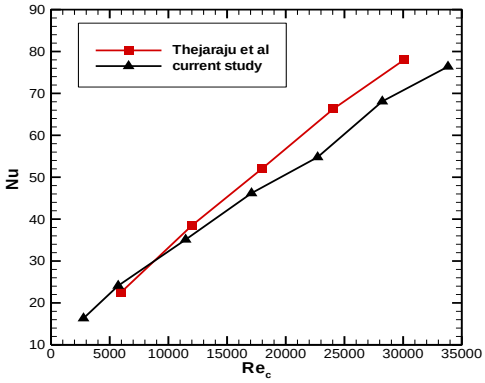

(a)

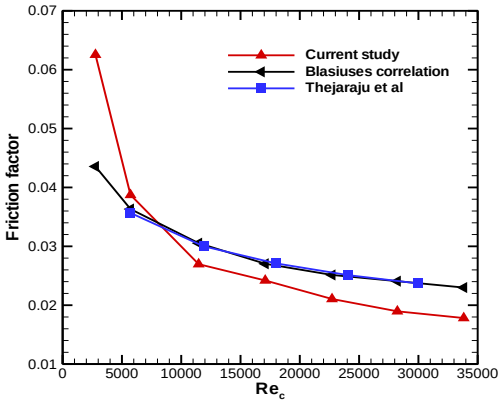

(b)

Figure 6. Validation of the current experimental setup; (a) Nusselt number with Thejaraju et al. [13], and (b) friction factor with the data of Thejaraju et al. and Blasius's correlation, $f = 0.316 \times Re^{-0.25}$.

6. Results and Discussion

In this study, an open-cell metalfoam having a porosity of 0.95 and 15 PPI were used to be filled in the space between the inner and outer pipes of the heat exchanger. The annulus heat exchanger involving smooth, full-filled, and partially/periodically-filled with MF were investigated experimentally. A wide turbulent range of Reynolds number was cover. The results were represented in terms of Nusselt number, friction factor, and PEC. The results were interpreted and analyzed as follows.

6.1 Thermal performance

6.1.1 Heat Transfer Coefficient

Figure (7) Shows the effect of Reynolds number on the Nusselt number of the cold air stream for all patterns proposed in this study. It can be seen that the smooth pattern showed the lowest Nu number while it increased with increasing Re number. Increasing Re number could increase the turbulence of the fluid, and then improve the mixing process of the fluid. An enhancement in the Nu number as observed when the MF was used in form of case 3 as D_{MF}/D_{pipe} = 0.75. This is due to compressibility behavior of the air which makes the air passes through the free gap (no MF) because of low flow resistance. Thus, the convection heat transfer between the air and the solid edges of the porous matrix reduces. Nevertheless, it is still higher than the smooth one.

Further enhancement in the Nu number was monitored when the MF was utilized as observed in case 4 and 5. It is worthy to be mentioned that case 4 filled 50% while case 5 filled 62.5% by MF. Nevertheless, case 4 provided greater heat transfer augmentation. Additional heat absorption by the MF was recorded in case 6 and 7. Case 7 showed higher heat transfer compared to case 6, whereas it filled 57.1% from the total annulus gap compared to 62.5% for case 6. Therefore, more heat dissipated was seen in case 7 due to the thermal boundary layer reattachment caused by zigzag MF configuration.

Case 2 showed the optimal heat dissipation compared to all the partially filled configurations, while it filled only 50% from the annulus gap. This is due to the fact that this configuration is attach at the developing thermal boundary layer region of the hot air stream and the wall temperature is at its higher value.

The maximum Nu number observed was found in case 1 as the whole annulus gap was completely filled with MF. Therefore, the air was forced through the MF and all the amount of the flow was in contact with the solid edges of the porous zone. It is worth to be mentioned that the behavior of the Nusselt number of this study is observed to be similar to the data published by [1, 5, 12, 13, and 14].

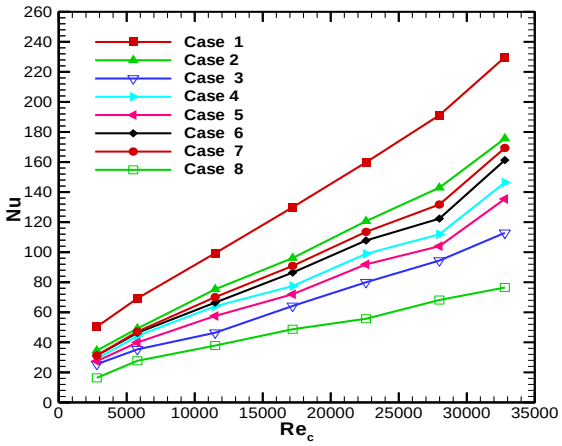

Figure 7. Effect of Reynolds number on the Nusselt number for all cases investigated in this study.

Figure 8(a) and 8(b) show the relationship between the average Nusselt number and the air ratio, AR, for all temperature differences considered here, ($\Delta T = T_{h\ in} - T_{c\ in}$) for case 1 and 8, respectively. The ΔT values between the inlet hot air and inlet cold air were 20, 30, 40, and 50°C. It was found that when the ΔT increased the Nu number increased and higher amount of heat can be absorbed by the cold air stream. In that case, the heat recovery increased and the heat loss to the ambient reduced.

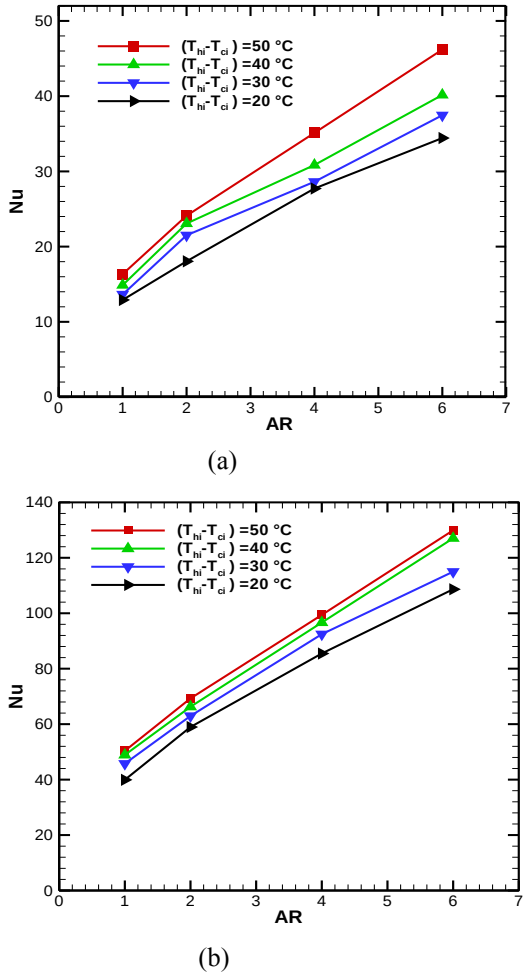

Figure 8. Effect of ΔT on the Nu number for several values of AR, (a) case 8, and (b) case 1.

Throughout the experiments, the local Nusselt number was calculated at the positions of 100, 250, and 400 mm from the beginning of the hot air stream at Re = 11,500 as shown in Figure 9. It can be noted that the local Nu number was affected strongly by the arrangement and configuration of the MF. This is due to the difference in values of the surface temperature and the temperature of the air flowing into the gap at the same distance and location on the test section.

In case 1, it was noticed a gradual increase in the value of local Nusselt number due to the use of MF along the test section and it reached the largest value at x = 400 mm. In case 2, it was noticed that the local Nu number was at x = 250 mm and then began to decrease due to the presence of MF in the second half of the test section, which could increase the mixing of air. The heat transfer between the pipe surface and the air, later began to decrease due to the absence of metal foam in the other half. For case 4, a slight increase was noticed in the local Nu due to the uniform distribution of the metal foam.

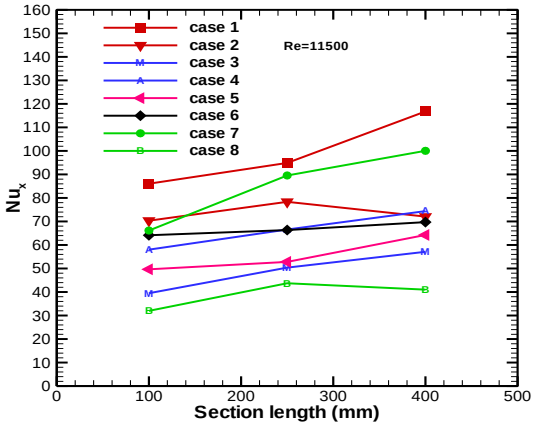

Figure 9. Effect of MF arrangement on the local Nusselt number at x = 100, 250, and 400 mm for all cases investigated in this study.

6.2. Hydraulic performance

The pressure drop associated with any fluid flow inside the pipelines is one of the major undesirable parameters that resulted due to the frictional losses between the fluid and the internal channel surfaces. It was observed that the pressure drop increased when the MF was used inside the flow channel as shown in Figure 10(a). The main goal of any researcher is to reduce the pressure drop as much as possible due to its negative effects such as high operating costs and low working life. It can be seen that the pressure drop exponentially with increasing the Re number due to high pumping power required to force the air through the porous media. In addition, the pressure drop was observed to be high according to how much the radial distance of the

annular gap was filled with metal foam and its thickness (i.e., length of the metal foam).

Figure 10(b) shows that the lowest friction factor observed was in case 8 in which no MF was used. Higher friction factor was recorded for case 3 as 75% of the annulus gap was filled with the MF. Although this filling ratio was the greatest compared to all other partially filling patterns, the friction factor was smaller than the others. This is attributed to the fact that 25% from the gap of the annulus stayed unfilled and it had the lowest flow resistance. Therefore, and due to the compressibility characteristic of the air, the most amount of air passed through the free passage while other amount flows through in the porous matrix. Case 5 only 12.5 MF washers (i.e., 125 mm) filled the gap completely while the other washers filled 0.75, 0.5, and 0.25 from the annulus gap. Therefore, this pattern also showed a low additional pressure drop. In addition, case 6 and case 7 also showed the same frictional losses as the number of washers having the radius ratio 1 was the same in both cases. Moreover, case 2 and case 4 displayed the same value of friction factor because they have the same number of washer that have a diameter ratio of 1. Thus, they provided an identical frictional resistance. It is worthy to saying that the full filled annulus with MF, led to a significant increase in the friction factor. When the air was forced through the porous zone and thus was additional pressure drop was reported. It is worth to be mentioned that the behavior of the pressure drop was similar to that reported by [1, 5, 12, 13, and 14].

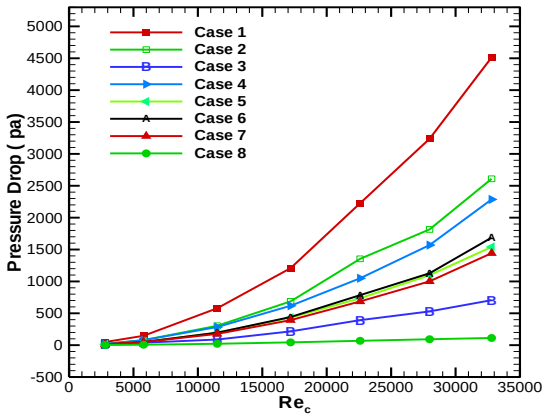

(a)

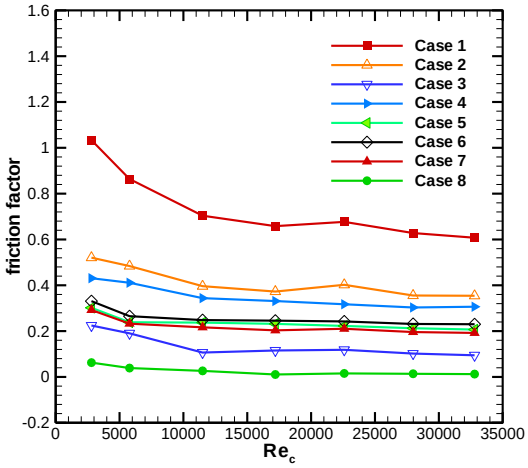

(b)

Figure 10. The variation of (a) pressure drop, (b) friction factor with Reynolds number.

6.3. Effectiveness of heat exchanger (E)

Figure 11 shows the influence of Reynolds number on the effectiveness of the double pipe heat exchanger for all cases studied in this paper. It was noticed that the effectiveness increased with the increase in the amount of cold air. It was found that the highest effectiveness was in case 1. When the gap between the two pipes was filled with metal foam, the lowest effectiveness was in case 8. It was also found that the effectiveness for case 7 was the optimal compared to all other cases except case 1. The reason for this behavior is due to the large mixing of cold air entering the gap between the two

pipes and to the surface area of contact provided by the metal foam.

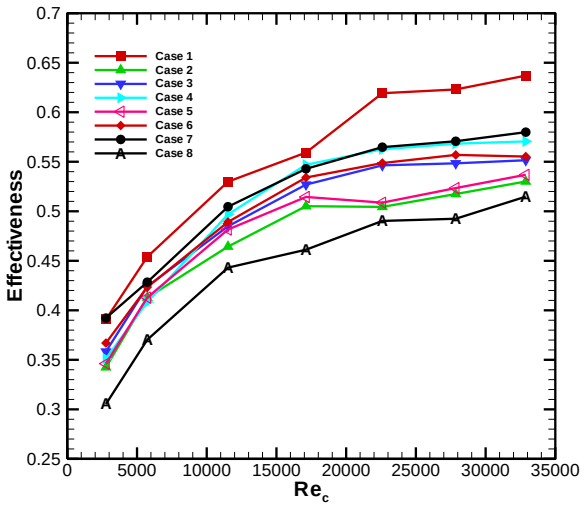

Figure 11. Effectiveness of all cases with the variation of Reynolds number.

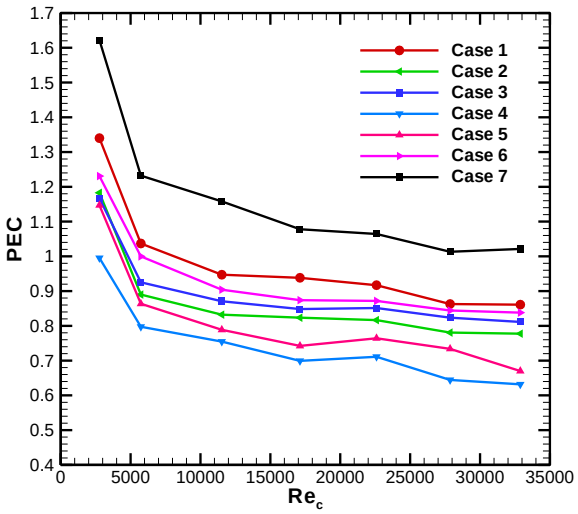

Figure 12. Performance evaluation criteria with the variation of Reynolds number.

7. Performance Evaluation Criteria (PEC)

It can be observed that the lowest PEC was in case 4 as shown in Figure 12. This case shows a moderate increase in the Nu number and moderate increase in the friction loss. The same trend was provided by case 5 as well. Case 3 provided a lower enhancement in the Nu number but so small increase in the friction factor, therefore, it provided higher PEC compared to the above cases. Greater PEC was also observed in case 2 due to high Nu and moderate friction factor. The PEC of case 2, 6, and 1 were close to each other. Although case 1 provided higher Nu number and higher pressure drop. A significant increase in the PEC was observed for case 7. This case showed the highest Nu compered to all cases filled partially with MF. All cases showed PEC ≥ 1 at low vales of Re number.

8. Conclusion

This study investigates experimentally the effect of metal foam arrangement on the heat transfer and pressure drop of double-pipe heat exchanger. Copper metal foam having 15PPI and porosity of 0.95 in different configurations installed in the gap of the annular space was investigated. The following conclusion can be drawn from the current study:

1- The temperature of the outer surface of the inner pipe was gradually decreased along the axial flow direction.

2- When the cold air flowrate increased, the convection heat transfer coefficient of the cold stream increased, and more enhancement was observed with using metal foam.

3- Higher Nusselt number was obtained when the metal foam was used, and the higher and lower Nu number ratio observed was 2.79 and 1.43 for case 1 and case 3 compared to case 8.

4- The pressure drop increased with increasing the flowrate particularly when the metal foam was used, while the pressure drop was strongly depended on the arrangement of the metal foam.

5- When the ΔT increased, the convection heat transfer coefficient increased, and in turn the Nusselt number increased as well.

6- The effectiveness of the heat exchanger was increased with the increase of the Reynolds number of

the cold air. The maximum effectiveness was 0.637 for case 1 at Re = 31,350.

7- The maximum PEC obtained was 1.62 for case 7 at Re = 2800.

Nomenclature

Symbol	Meaning	Units
A_i	Surface area of inner copper pipe	m^2
A_o	Surface area of the annular gap	m^2
d_i	Diameter of inner copper pipe	m
d_o	Diameter of outer copper pipe	m
D_i	Diameter of inner (PVC) pipe	m
D_o	Diameter of inner (PVC) pipe	
D_h	Hydraulic diameter of annular	m
h_c	Convection heat transfer coefficient of cold air	$W/m^2 K$
h_h	Convection heat transfer coefficient of hot air	$W/m^2 K$
k	Thermal conductivity of fluid	W/m K
Q	Heat transfer	W
f	friction factor	-------
$\dot{m}$	mass flow rate	kg/s
u	Velocity	m/s
V	volume of air	m^3/s
cp	Specific heat at constant pressure	kJ/kg
T	Temperature	°C
Re	Reynolds number	-------
T_{ho}	Outlet temperature of hot air	(°C)
$T_{c\,avg}$	average temperature of cold air	(°C)
T_{ci}	Inlet temperature of cold air	(°C)
T_{co}	Outlet temperature of cold air	(°C)
$T_{s_{avg}}$	average surface temperature of inner pipe	(°C)
E	Effectiveness	
Nu_{mf}	Nusselt number with metal foam	
Nu_s	Nusselt number without MF	
f_{mf}	Friction factor with metal foam	
f_s	Friction factor without metal foam (smooth)	

Greek symbols

ρ	Density	kg m
μ	Viscosity of air	Pa.s
g	gravitational acceleration	m/s^2
Δh	Pressure head	mm
ΔP	Pressure drop	Pa
ρ	Density	kg m
μ	Viscosity of air	Pa.s
g	gravitational acceleration	m/s^2
Δh	Pressure head	mm

Abbreviation

PPI	Pores per inch
PEC	Performance Evaluation Criteria
MF	Metal foam
i	Inlet
o	Outlet
PVC	Polyvinyl chloride

References

[1] J. A. Hamzah and M. A. Nima, "Experimental Study of Heat Transfer Enhancement in Double-Pipe Heat Exchanger Integrated with Metal Foam Fins," Arab. J. Sci. Eng., vol. 45, no. 7, pp. 5153–5167, 2020, doi: 10.1007/s13369-020-04371-3.

[2] N. Targui and H. Kahalerras, "Analysis of fluid flow and heat transfer in a double pipe heat exchanger with porous structures," Energy Convers. Manag., vol. 49, no. 11, pp. 3217–3229, 2008, doi: 10.1016/j.enconman.2008.02.010.

[3] H. Kahalerras and N. Targui, "Numerical analysis of heat transfer enhancement in a double pipe heat exchanger with porous fins," Int. J. Numer. Methods Heat Fluid Flow, vol. 18, no. 5, pp. 593–617, 2008, doi: 10.1108/09615530810879738.

[4] A. Jamarani, M. Maerefat, N. F. Jouybari, and M. E. Nimvari, "Thermal Performance Evaluation of a Double-Tube Heat Exchanger Partially Filled with Porous Media Under Turbulent Flow Regime," Transp. Porous Media, vol. 120, no. 3, pp. 449–471, 2017, doi: 10.1007/s11242-017-0933-x.

[5] H. R. Abbasi, E. Sharifi Sedeh, H. Pourrahmani, and M. H. Mohammadi, "Shape optimization of segmental porous baffles for enhanced thermo-hydraulic performance of shell-and-tube heat exchanger," Appl. Therm. Eng., vol. 180, p. 115835, 2020, doi: 10.1016/j.applthermaleng.2020.115835.

[6] Isbeyeh W. Maid , Kifah H. Hilal, Jawaher K. Hassun" experimental study of heat transfer enhancement in heat exchanger using porous media"G lobal J ournal of E ngineering S cience and R esearch M anagement," vol. 4, no. 9, pp. 82–91, 2017, doi: 10.5281/zenodo.886915

[7] U. K. N. Madhav Mishra, "Experimental Investigations of Double Pipe Heat Exchanger With Triangular Baffles," Int. Res. J. Eng. Technol., vol. 03, no. 08, pp. 1137–1141, 2016.

[8] K. Nawaz, J. Bock, and A. M. Jacobi, "Thermal- hydraulic performance of metal foam heat exchangers under dry operating conditions," Appl. Therm. Eng., vol. 119, pp. 222–232, 2017, doi: 10.1016/j.applthermaleng.2017.03.056.

[9] H. J. Xu, Z. G. Qu, and W. Q. Tao, "Numerical investigation on self-coupling heat transfer in a counter-flow double-pipe heat exchanger filled with metallic foams," Appl. Therm. Eng., vol. 66, no. 1–2, pp. 43–54, 2014, doi: 10.1016/j.applthermaleng.2014.01.053.

[10] A. A. Sertkaya, K. Altinisik, and K. Dincer, "Experimental investigation of thermal performance of aluminum finned heat exchangers and open-cell aluminum foam heat exchangers," Exp. Therm. Fluid Sci., vol. 36, pp. 86–92, 2012, doi: 10.1016/j.expthermflusci.2011.08.008

[11] A. Nasser, Adel Alhusseny and A. Turan, "Rotating metal foam structures for performance enhancement of double-pipe heat exchangers," Int. J. Heat Mass Transf., vol. 105, pp. 124–139, 2017, doi: 10.1016/j.ijheatmasstransfer.2016.09.055.

[12] M. R. Salem, M. K. Althafeeri, K. M. Elshazly, M. G. Higazy, and M. F. Abdrabbo, "Experimental investigation on the thermal performance of a double pipe heat exchanger with segmental perforated baffles," Int. J. Therm. Sci., vol. 122, no. 02, pp. 39–52, 2017, doi: 10.1016/j.ijthermalsci.2017.08.008

[13] R. Thejaraju, K. B. Girisha, S. H. Manjunath, and B. S. Dayananda, "Experimental investigation of turbulent flow behavior in an air to air double pipe heat exchanger using novel para winglet tape," Case Stud. Therm. Eng., vol. 22, no. December, p. 100791, 2020, doi: 10.1016/j.csite.2020.100791.

[14] S. P. Govindani, "Experimental Analysis of Heat Transfer Enhancement in a Double Pipe Heat Exchanger Using Inserted Rotor Assembled Strand," Volume: 03 Issue: 01 | Jan-2016.

[15] H. Arasteh, M. R. Salimpour, and M. R. Tavakoli, "Optimal distribution of metal foam inserts in a double-pipe heat exchanger," Int. J. Numer. Methods Heat Fluid Flow, vol. 29, no. 4, pp. 1322–3142, 2019, doi: 10.1108/HFF-04-2018-0162.

[16] Incropera F.P,"Fundamentals of Heat and Mass Transfer: 6th ed. Notre Dame, Indiana, JOHN WILEY, Son.2005.

[17] S. J. Kline, "Describing uncertainty in single sample experiments," Mech. Eng., vol. 75, pp. 3–8, 1953.